

# Processing of Semipolar and Nonpolar InGaN Based Laser Diodes

Robert A.R. Leute

*We studied a fabrication process suitable for laser diodes based on both nonpolar and semipolar AlGaInN structures. The simplicity of the designated device architecture of an oxide stripe laser is well suited as a test structure. We investigate the crucial process of resonator formation for nonpolar material and describe the response of nonpolar material to dry etching.*

## 1. Introduction

Laser diodes (LDs) based on InGaN quantum well (QW) structures emitting in the blue to green spectral region are of great interest for applications ranging from spectroscopy to laser projectors for mobile devices. Whereas LDs in the blue spectral region are available commercially, the so-called “green gap” is just at the point of being bridged. The necessity of creating InGaN QWs with high indium content in order to achieve longer wavelengths leads to an aggravation of epitaxial challenges. Optimal growth conditions for the active region become increasingly different from the surrounding GaN layers with increasing In content. Furthermore, the lattice mismatch between GaN and InGaN induces strong polarization fields along the commonly used polar directions, thus resulting in a reduced recombination rate, due to the quantum confined Stark effect (QCSE). The QCSE draws the wave functions of electrons and holes apart, thereby decreasing the wave function overlap. This inherent issue can be avoided or alleviated by the growth of the active region on nonpolar or semipolar planes [1].

There is no consensus nor clear scientific indication about the most opportune crystal plane yet. The longest wavelengths (520-531 nm) have been achieved on the semipolar  $\{20\bar{2}1\}$  plane [2,3] while LDs on the conventional c-plane have been pushed as far as 515 nm [4, 5]. The essential issues of increasing the indium incorporation and reducing defect densities are still unsolved. Additionally, differently oriented samples pose new challenges for device processing, too. Especially the alignment of laser mirrors in respect to crystal planes is drastically changed when growing devices with alternate crystal orientations. We investigate the subsequent material response in respect of differences between polar and nonpolar samples.

### 1.1 Fabrication process for an oxide-stripe laser

There are numerous device architectures for laser diodes. Aim of our investigations is the application of an oxide stripe laser diode fabrication process on nonpolar and semipolar

samples. The edge emitting design of an oxide-stripe laser is well established and was already applied successfully to conventional c-plane samples, producing a laser diode with a threshold current density of  $6 \text{ kA/cm}^2$  [6]. Fig. 1 shows the LD schematically.

Vertical optical confinement is achieved by sandwiching the active layer between two AlGaN layers with lower refractive indices. Laterally, the current injection along a small opening in the insulating oxide layer pumps just a narrow region leading to gain guiding. Lateral optical confinement is achieved by isolating the top metal contact from the laser structure except for a small stripe opening.

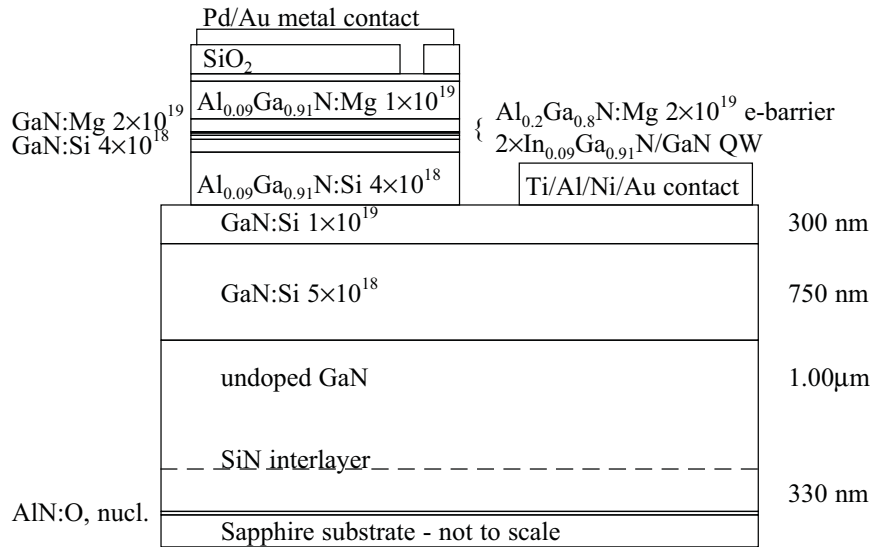
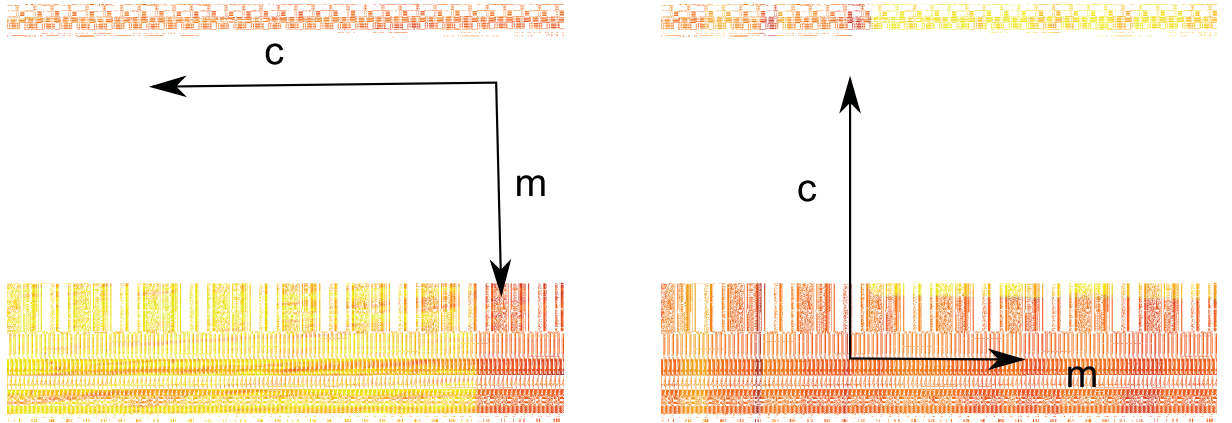


Fig. 1: Epitaxial structure and layout of laser device.

## 2. Experimental

The processing steps were investigated using test samples that were *not* laser structures. The efficiency of the laser diodes is reliant on the reflectivity and orientation of the resonator mirrors. Conventional LDs based on polar AlInGaN samples have typically resonator facets formed by m and a oriented crystal planes. Thus they are well aligned and very smooth. For homoepitaxially grown samples (e.g. [3]) as well as samples grown on SiC this can be achieved by cleaving. For heteroepitaxial growth on sapphire, the crystal orientation between substrate and the grown layers is rotated and cleaving of the substrate will not result in equally cleft layers.

Therefore etching is used for resonator formation. In order to get steep and smooth sidewalls, we need both an etching mask material with high selectivity as well as an etching method with high anisotropy. The former is fulfilled by nickel (cf. [7]). For the latter, solely dry etching methods such as reactive ion etching (RIE) are utilized. Especially the possibility to balance physical and chemical etching gives control of the etching profile in contrast to wet etching. The high anisotropy is especially needed for



**Fig. 2:** Optical microscope image (200 $\times$ ) of Ni mask aligned along  $c$ -axis for HVPE (left) and MOVPE (right) grown samples.

semipolar samples where aspired resonator facets no longer coincide with low index crystal facets.

The alignment of the resonators has great influence on the gain of the diode, especially for semipolar and nonpolar samples. Scheibenzuber et al. [8] calculated gain and optical eigenmodes in InGaN laser diodes and found substantially higher gain values for laser ridges oriented parallel to the  $c$ -axis (or its projection) compared to an orientation perpendicular to it. Thus, it is necessary to fabricate resonators along the  $c$ -axis. Resonator sidewalls will then be formed by  $c$ -planes and  $m$ -planes for  $a$ -plane oriented samples. As mentioned before, prospective samples will be grown heteroepitaxially on sapphire substrates and thence will be unsuited to create mirrors by means of cleaving.

For testing, two samples were prepared. The first sample S9456aGSr consists of  $\approx 5.46 \mu\text{m}$  nominally undoped  $a$ -plane oriented GaN grown by MOVPE. The second sample V9081\_7 consists of a MOVPE grown  $a$ -plane oriented GaN template, overgrown inside a hydride vapor phase epitaxy (HVPE) reactor creating an approximately  $20 \mu\text{m}$  thick  $a$ -plane oriented nominally undoped GaN layer. Both samples were grown on  $r$ -plane sapphire and show typical grooves (cf. [9]) along  $c$ -direction. 300 nm nickel was evaporated as etch-

**Table 1:** RIE conditions used for dry etching of  $a$ -plane GaN.

Electrode RF power	50W
Pressure	15 mTorr
Cl <sub>2</sub>	1.7 sccm
BCl <sub>3</sub>	10.2 sccm
Ar	5.1 sccm
Etch rate	$\approx 40 \text{ nm/min}$

mask using 15 nm titanium as an adhesion layer. A mesa pattern was transferred by photolithography. The alignment of the stripes along the  $c$ -direction can be seen in Fig. 2. Under the optical microscope, the grooves and the overall roughness are clearly visible.

For a-plane samples, the resonator edges are aligned parallel to  $\{0001\}$  and  $\{10\bar{1}0\}$  crystal planes, we therefore expect smooth and steep sidewalls. On both samples mesa structures were etched with an Oxford Plasmalab 100 RIE system using the parameters given in table 1. The parameters were chosen from previous experiences with c-plane samples [6] where sidewalls with an inclination angle of  $80^\circ$  were achieved.

After dry etching the mask was removed with a wet etching solution of  $\text{H}_2\text{O}$ ,  $\text{HCl}$  and  $\text{H}_2\text{O}_2$ . The samples were then investigated with a scanning electron microscope (SEM).

### 3. Results

The aforementioned roughness of heteroepitaxially grown nonpolar samples complicated the deposition of the nickel etch mask. The 300 nm thick Ni layer is highly strained and even with a Ti adhesion layer, the reduced contact to the GaN surface lead to flaking and self separation of the mask from the sample. In order to improve adhesion and reduce the strain, we increased the thickness of the Ti layer from 15 nm to 20 nm and introduced two 1 nm thick gold interlayers each after 100 nm of nickel for strain relaxation. Thusly evaporated etch masks showed flawless adhesion and allowed smooth structuring. The etch time (RIE) was chosen for an etching depth of approximately  $1.2\ \mu\text{m}$  based on previous experiences with c-plane GaN. We found no noticeable difference in etch rate for the a-plane samples. Figure 3 shows the SEM picture of a mesa flank of the HVPE grown sample with included height measurement. The etching depth of the MOVPE grown sample was found to be the same within the accuracy of the measurement (not shown). Both samples show a humpy roughening of the upper half of the flank but are smooth below (Fig. 5). Whether these bulges are related to material properties or caused by the processing is unclear, yet.



**Fig. 3:** SEM picture of mesa side flank (HVPE sample), height  $\approx (1.2 \pm 0.1)\ \mu\text{m}$ .

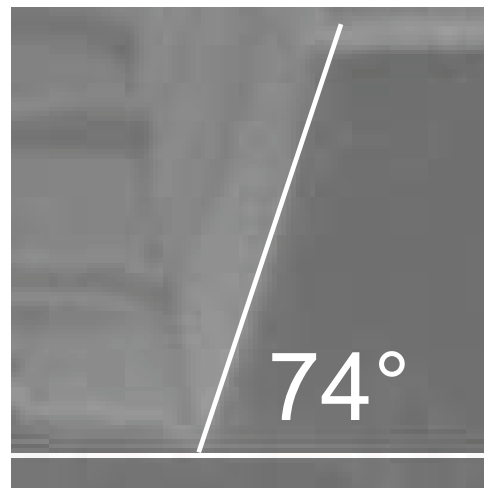


**Fig. 4:** SEM picture (detail) of cleft mesa, considering the viewpoint the inclination angle is  $\approx (74 \pm 2)^\circ$  (MOVPE sample).

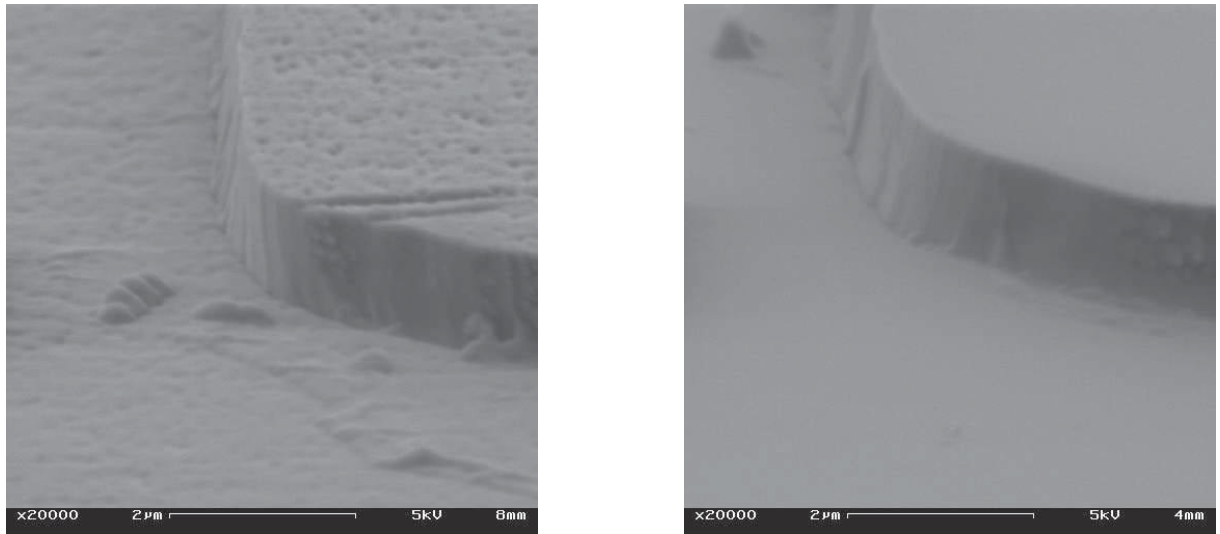


**Fig. 5:** SEM images of the mesa edge for HVPE (left) and MOVPE (right) grown a-plane GaN after removal of the Ni mask.

Measurement on a mesa cleft (Fig. 4) shows an inclination of only  $72^\circ$  to  $75^\circ$ . Further optimization of the anisotropy of the etching process deems necessary, before they can be used as resonator mirrors.

The etching seemed to have only marginally deleterious effects on the etched surface. They still show a typical respective smoothness for HVPE and MOVPE grown a-plane GaN (Fig. 6) and hence appear well suited for further processing steps.

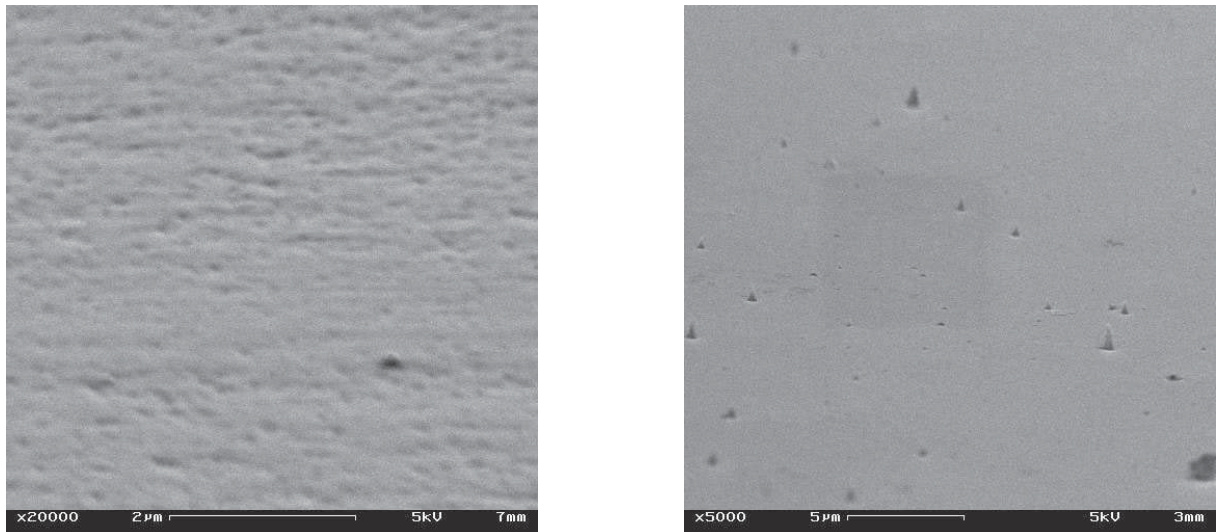


**Fig. 6:** SEM images of etched surface for HVPE (left) and MOVPE (right) grown a-plane GaN.

#### 4. Conclusion & Outlook

The response of nonpolar GaN to RIE dry etching was investigated. The etching mask was optimized by introducing gold interlayers for a high reproducibility and reliability. While

etching depth and profile are very promising further investigations for a-plane samples are needed to increase the inclination angle of the etched resonator mirrors as well as further experiments on samples with semipolar surfaces.

## Acknowledgments

Much valued technical support was given by Ilona Argut, Rudolf Rösch and Rainer Blood.

## References

- [1] P. Waltereit, O. Brandt, A. Trampert, H.T. Grahn, J. Menniger, M. Ramsteiner, M. Reiche, and K.H. Ploog, “Nitride semiconductors free of electrostatic fields for efficient white light-emitting diodes”, *Nature*, vol. 406, pp. 865–868, 2000.
- [2] Y. Enya, Y. Yoshizumi, T. Kyono, K. Akita, M. Ueno, M. Adachi, T. Sumitomo, S. Tokuyama, T. Ikegami, K. Katayama and T. Nakamura, “531 nm green lasing of InGa<sub>N</sub> based laser diodes on semi-polar {20 $\bar{2}$ 1} free-standing GaN substrates”, *Appl. Phys. Express*, vol. 2, p. 082101, 2009.
- [3] Y. Yoshizumi, M. Adachi, Y. Enya, T. Kyono, S. Tokuyama, T. Sumitomo, K. Akita, T. Ikegami, M. Ueno, K. Katayama, and T. Nakamura, “continuous-wave operation of 520 nm green InGa<sub>N</sub>-based laser diodes on semi-polar {20 $\bar{2}$ 1} GaN substrates”, *Appl. Phys. Express*, vol. 2, p. 092101, 2009.
- [4] T. Miyoshi, S. Masui, T. Okada, T. Yanamoto, T. Kozaki, S. Nagahama, and T. Mukai, “510–515 nm InGa<sub>N</sub>-based green laser diodes on c-plane GaN substrate”, *Appl. Phys. Express*, vol. 2, p. 062201, 2009.
- [5] A. Avramescu, T. Lerner, J. Müller, S. Tautz, D. Queren, S. Lutgen, and U. Strauss, “InGa<sub>N</sub> laser diodes with 50 mW output power emitting at 515 nm”, *Appl. Phys. Lett.*, vol. 95, p. 071103, 2009.
- [6] M. Fikry, *Epitaxy and Processing of AlGaInN Heterostructures for Light Emitting Diode Applications*, Master Thesis, Ulm University, Ulm, Germany, 2008.
- [7] S.A. Smith, C.A. Wolden, M.D. Bremser, A.D. Hanser, R.F. Davis, and W.V. Lampert, “High rate and selective etching of GaN, AlGa<sub>N</sub>, and AlN using an inductively coupled plasma”, *Appl. Phys. Lett.*, vol. 71, pp. 3631–3633, 1997.
- [8] W.G. Scheibenzuber, U.T. Schwarz, R.G. Veprek, B. Witzigmann and A. Hangleiter, “Calculation of optical eigenmodes and gain in semipolar and nonpolar InGa<sub>N</sub>/Ga<sub>N</sub> laser diodes”, *Phys. Rev. B*, vol. 80, p. 115320, 2009.
- [9] T. Detchprohm, M. Zhu, Y. Li, Y. Xia, L. Liu, D. Hanser, C. Wetzel, “Growth and characterization of green GaIn<sub>N</sub>-based light emitting diodes on free-standing non-polar GaN templates”, *J. Crystal Growth*, vol. 311, pp. 2937–2941, 2009.